IN SITU INFRARED SPECTROELECTROCHEMISTRY: APPLICATIONS TO ELECTROCATALYSIS

M.I.S. Lopes and L. Proença

CECUL, Faculdade de Ciências da Universidade de Lisboa, R. da Escola Politécnica 58, 1294 Lisboa Codex, Portugal.

Abstract

The use of *in situ* infrared (IR) vibrational spectroscopy on the elucidation at a molecular level of electrochemically induced phenomena, *i.e.*, *in situ* IR spectroelectrochemistry, has been rapidly developing in the last two decades, since a pioneer work of Bewick *et al.*, by using modulation and synchronous detection of the signal in external reflectance IR spectroscopy.

In situ IR spectroelectrochemistry has been proved to be a powerful tool for investigation of the electrode|solution interface, namely by providing information on the structural, bonding and dynamical properties of adsorbate species on electrode surfaces, on the behaviour of supporting electrolyte and solvent molecules at the electrochemical interface and also on reaction mechanisms and kinetics of electrocatalytic reactions.

An overview of some theoretical aspects of IR reflectance spectroscopy is presented and experimental details of some *in situ* techniques are described, namely EMIRS (Electrochemically Modulated Infrared Reflectance Spectroscopy), SNIFTIRS (Subtractively Normalised Interfacial Fourier Transform Infrared Reflectance Spectroscopy) and SPAIRS (Single Potential Alteration Infrared Reflectance Spectroscopy). A few selected applications of these techniques to electrocatalysis are also presented.

1. Introduction

The use of *in situ* IR spectroscopy for studying electrode processes was first introduced in the sixties, using internal reflectance techniques [1], in an effort to provide a better elucidation of the electrode|solution interface at a molecular level. This Attenuated Total Reflection (ATR) method minimises solvent absorbance but sensitivity is limited and the choice of electrode material is restricted because there are few materials that are both electronically conductive and transparent to IR radiation. Further improvements have made the ATR method useful for many investigations on thin metal films.

The strong absorption of IR radiation by solvents was long considered to be an insuperable obstacle to *in situ* IR spectroscopy at electrode surfaces in the external reflection mode. However, at the beginning of the eighties, Bewick *et al.* [2] demonstrated that the use of sophisticated modulated spectroscopic techniques could lead to the *in situ* detection of adsorbates formed at an electrode|aqueous solution interface, even at a submonolayer level. Since that, there has been a considerable development of different *in situ* IR reflectance techniques, each of them having their own peculiarities and limits [3]. New fields of application have been investigated and decisive progresses have been made mostly in terms of increased sensitivities and reduced spectral acquisition times. External reflectance IR spectroelectrochemical methods are generally more popular than ATR methods because they are more versatile and they can be performed either on smooth polycrystalline bulk metals or single crystal electrode surfaces.

Plenary lecture presented at the VIII Meeting of The Portuguese Electrochemical Society, Covilhã, Portugal (1996) and dedicated to Bernard Beden who by his scientific and human qualities has greatly contributed to the development of *in situ* spectroelectrochemistry.

In situ IR spectroelectrochemical methods have been extremely useful for a variety of surface studies but they can be applied to investigations of solution species as well as to species on electrode surfaces. Many types of electrode substrates have been used in IR spectroelectrochemical experiments, including well defined single crystals, semiconductors, chemically modified electrode surfaces, thin metal films, oxide layers, and numerous polycrystalline bulk metals.

In the following sections an overview of some theoretical aspects of IR reflectance spectroscopy and of some now current (but not yet "routine") *in situ* IR spectroscopic techniques and their appropriate fields of application – with a special emphasise on electrocatalysis – will be outlined. Some examples will be given either taken from our work or from the literature.

2. Absorption-Reflection Spectroscopy

In this section some basic principles of absorption-reflection spectroscopy and of some *in situ* spectroelectrochemical techniques will be described. For further details the reader is invited to consider, among others, references [3 – 8].

2.1. Basic considerations

There are two important points to keep in mind when considering reflectance spectroscopy:

(*i*) The first one is that, at variance with conventional transmission spectroscopy, one has to consider two limit cases where the reflecting surface is either free, or covered by a layer of adsorbing species (Fig. 1). Thus, instead of the commonly known Lambert-Beer's law $I=I_0\exp(-\alpha x)$, where I_0 and I are the intensities of the light before and after crossing a layer x of an absorbing medium (whose absorption coefficient is α), it is the relative change of reflectivity $\Delta R/R$ which is considered.

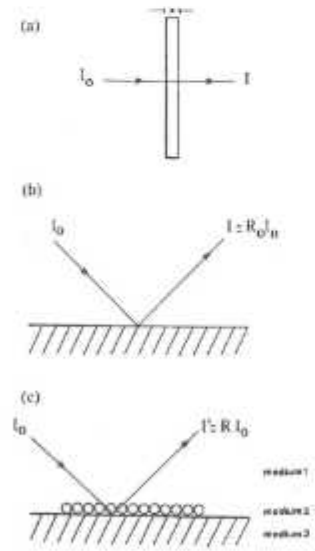

Figure 1. Transmission (a) and reflectance (b) modes on a bare surface or on a surface covered by an adsorbing layer (c).

Actually, if R_0 is the reflectivity of the bare surface, R the reflectivity of the covered surface, I and I' the intensities of the emerging beam after reflection in the two preceding cases, and owing to the fact that normally $R<R_0$, then it comes :

$$\frac{\Delta R}{R_0} = \frac{R - R_0}{R_0} = \frac{I'-I}{I} = \frac{I'}{I} - 1$$

Therefore the variation of absorbance, ΔA, can be written as :

$$\Delta A = \log I_0/I' - \log I_0/I = - \log (1 + \Delta R/R_0)$$

or, finally, as $\Delta R << R_0 \sim R$,

$$\boxed{\Delta A = - \frac{\Delta R}{R}}$$

For experimental convenience it is the relative change of reflectivity, $\Delta R/R$, which is measured, and not ΔA. This is the reason why the technique was called *absorption-reflection spectroscopy*.

(*ii*) The second point to bear in mind concerns the effect of the optical polarisation of the beam.

Let us consider the polarisation plane perpendicular to the electrode surface, commonly referred as "p" polarisation at variance with "s" polarisation for the planes parallel to the surface. When an electromagnetic wave crosses a solution (of refractive index n_1 and extinction coefficient k_1) and reflects upon a metallic surface (of optical constants n_2, k_2), there is no phase shift of the p-component of the electric field vector, E, provided that the incidence angle φ_1 is high enough (Fig. 2). More precisely, if φ_2 is the refraction angle associated with φ_1 through the so-called Descartes' (or Snelius') law, $n_1\sin\varphi_1 = n_2\sin\varphi_2$, φ_1 has to be high enough for the equation $\varphi_1 + \varphi_2 > \pi/2$ to be satisfied.

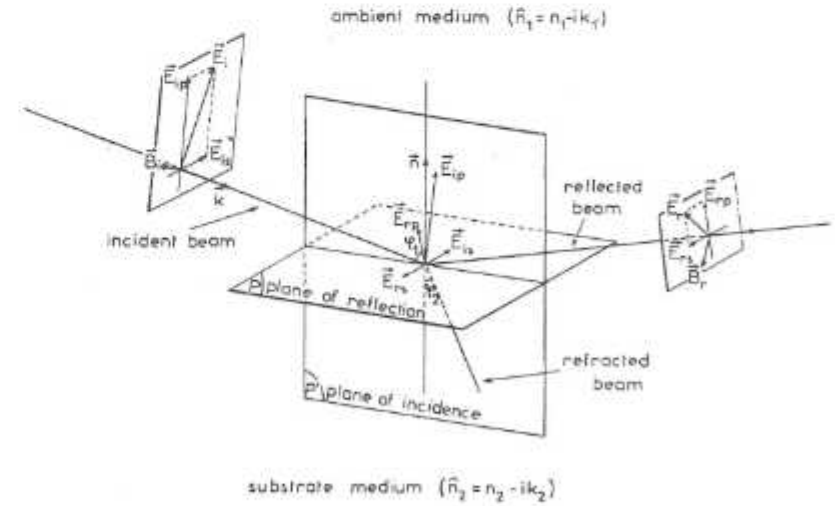

Figure 2. Reflection of an electromagnetic wave (E, B) upon a metal surface.

Interestingly, if E_{ip} and E_{rp} are the incident and the reflected p-components of the electric field vector, respectively, then they co-add at the point of reflection, so that the magnitude of E_p, the resulting vector, is greater (up to nearly twice) than that of E_{ip}. In contrast, E_{is} and E_{rs} always subtract, whatever the incidence angle is, so that the resulting vector E_s is always small. This is illustrated in Fig. 3 where E_p is decomposed in two components, $E_{p\perp}$, perpendicular to the plane of reflection, and $E_{p=}$, parallel to the plane of reflection.

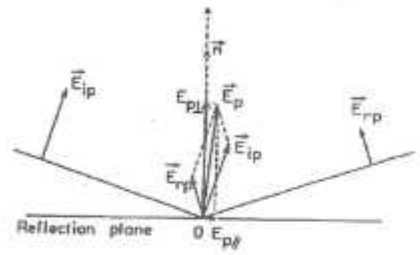

Figure 3. Resulting vector E_p at the reflection plane of a metal surface.

At high angles of incidence $E_{p\perp}$ can be nearly doubled whereas $E_{p=}$ remains always very small, like E_s (Fig. 4).

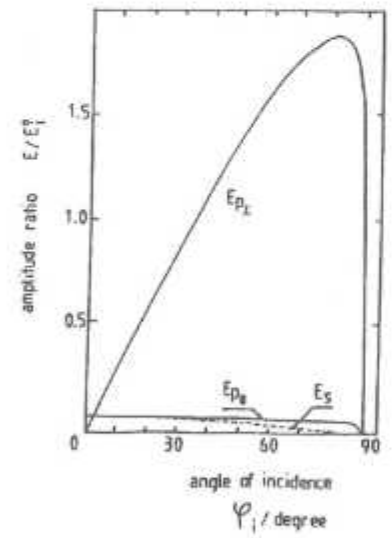

Figure 4. Dependence of E_p and E_s on the angle of incidence φ_i, for highly reflecting metals, in the near infrared.

The main consequence of this is the so-called "surface selection rule": *only the species which have a non zero dipole moment perpendicular to the surface (or nearly so) will have the ability to absorb the radiation*. In more simple words, it means that molecules adsorbed flat on the surface will have very little chance to be detected by vibrational reflectance spectroscopy. This additional "rule" is not a true selection rule because no quantum numbers are involved but it allows to deduce the orientation of molecules adsorbed at the surface electrode. Another consequence of these

features is that the maximum absorption of the infrared beam will occur for p-polarised light. This justifies that p-polarisers are usually used in reflectance spectroscopy.

2.2. Reflection modes

Two modes can be considered. They lead to different designs of cells.

(*i*) In the internal reflection mode (Fig. 5b) the beam arrives through an IR transparent substrate (Ge, Si, ...) and which serves as window. On top of it, a thin layer of the metal of interest (Pt, Au, Fe, Cd, ...) has to be deposited for serving as working electrode. One or several reflections can be made according to the shape of the substrate and to the angle of incidence of the beam. Energy absorption by the solvent is therefore avoided but the technique is restricted to the study of evaporated films whose catalytic behaviour may be very different from that of smooth metals or single crystals.

(*ii*) In the external reflection mode (Fig. 5a) there is no restriction on electrode thickness and therefore any surface can be investigated (smooth, rough, polycrystalline or single crystal, modified by adatoms, ...).The beam crosses the transparent infrared window and a very thin (a few microns) electrolyte layer, before being reflected by the electrode surface and crossing back again the solution and the window.

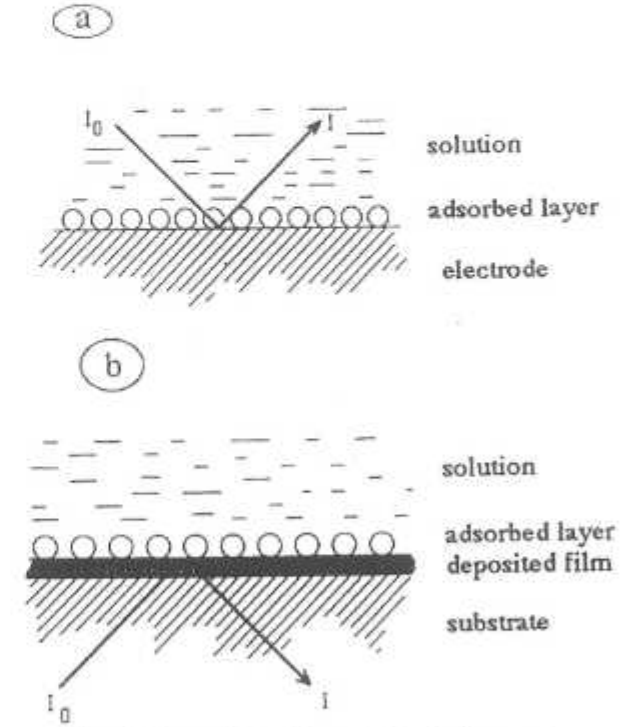

Figure 5. External (a) and internal (b) reflection modes.

A limited number of materials are available for the window, CaF_2, Si and ZnSe being those most frequently used. The flatness of the window and of the working electrode, which together determine

the minimum thickness of the solution layer, and the incident angle of the infrared beam are very critical parameters. Depending on the refractive indices of window materials and solutions, angles of incidence of 65° for CaF_2, or 70° for Si are acceptable compromises between the high incidence angles necessary to maximise the resulting electric field vector at the interface, E_p (*i.e.*, parallel to the incidence plane), and the low incidence angles necessary to avoid too much loss of energy by reflection on the outer surface of the flat window. As for the solution layer, an average thickness of a few micrometers (with aqueous solutions) allows to maintain the electrochemical control of the interface without too much infrared radiation being adsorbed. However, when the electroactive species is consumed by the reaction during spectral accumulation, severe mass transfer limitations can occur in the thin layer of electrolyte. This does not happen when the adsorption equilibrium is realised before spectral accumulation and provided that the potential limits of the modulation signal are well chosen within the adsorption potential domain.

Fundamentally the two reflection modes should be equivalent. In practice, however, the restrictions due to materials and the nature of adsorbing material make them different, not only for the design of spectroelectrochemical cells, but also for the type of results.

The first cell used in external reflection IR spectroelectrochemistry has seen a number of refinements and improvements. Fig. 6 shows the design of an external reflectance IR cell .

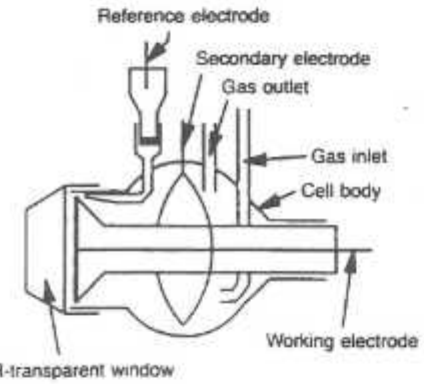

Figure 6. Configuration of an external reflectance cell for IR spectroelectrochemistry.

2.3. Types of spectrometers

The first *in situ* IR experiments in the absorption-reflection method used grating spectrometers requiring the modulation of the electrode potential during the measurement of the spectrum. Prisms or grating monochromators allow the observation of a narrow frequency domain during the spectrum recording which is determined by the width of the exit slit. Thus, grating spectrometers have serious limitations in the energy throughput, particularly at high resolution, when very narrow slits are required. Further improvements to maximisation of energy throughput and of detectability were achieved and variants were developed by modulating the state of polarisation of light (s-p modulation) while keeping the electrode at constant potential.

The most important improvements were achieved by the use of Fourier Transform Infrared (FTIR) instruments. The high rate of collection of spectra in this case makes unnecessary the modulation of potential, thus giving the possibility of collecting spectra during the application of

any desired potential program. A FTIR spectrometer is based on the use of an interference pattern resulting from the passage of polychromatic radiation from an IR source through a Michelson interferometer. After passing through the interferometer, the beam reaches the sample and its interference pattern change because of the absorption of radiation by the sample. The signal is then detected by a phase-sensitive detector (PSD) and finally decoded by means of a Fourier transform calculation. The result of this operation is an ordinary single beam spectrum.

The number of groups using FTIR spectroscopy is growing continuously owing to the development of instrumentation, to high throughput of radiation and to its "multiplex advantage", since the detector is viewing all the frequencies all the time during the measurement, enhancing the signal-to-noise ratio (S/N).

A schematic diagram for *in situ* IR spectroelectrochemical experiments is shown in Fig. 7.

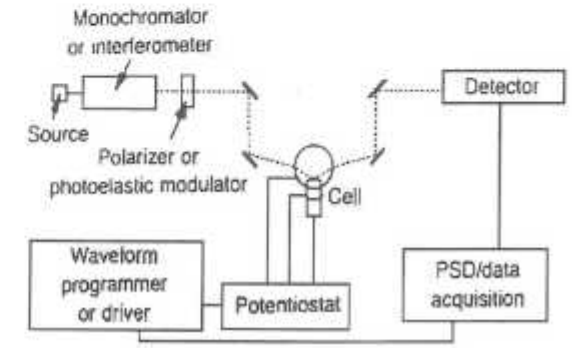

Figure 7. Schematic diagram of the instrumentation for IR spectroelectrochemistry.

2.4. Signal enhancement

A large contribution to the success of IR reflectance spectroscopy at the electrode|electrolyte interface results from the coupling of spectroscopic and electrochemical techniques. Furthermore, due to the strong absorption of the solvent and the subsequent weakness of the emerging beam, it is indispensable to use extremely powerful additional techniques to extract the signals corresponding to surface species from that arising from bulk species. Therefore, in addition to the spectrometer itself and controlling computer, equipment is required firstly to monitor the electrochemical processes occurring at the metal|solution interface (e.g., a potentiostat and a waveform generator) and secondly to enhance the weak signal-to-noise ratio, inherent to this type of experiments, prior to its storage and processing.

Usually, the signals in phase with a reference modulation are detected with a phase-sensitive detector and/or an averaging system, followed by suitable signal processing (spectral accumulation and averaging or spectral subtraction) with microcomputer programs.

2.5. Main *in situ* infrared reflectance spectroscopic techniques

The variants of IR reflectance spectroscopy differ on the type of spectrometer employed, on the reflection mode and, principally, on the technique used for signal enhancement, without which no signals due to adsorbed species can be extracted. The main IR reflectance techniques are listed in Table 1, together with references to early works. Basic principles of these techniques are described in references [3, 4]. Experimental details are given in the original references listed in the Table.

Table 1 - Characteristics of the main infrared reflectance techniques

Type of spectrometer	Signal enhancement technique	Reflection mode	Name of techniques*	References
Dispersive	Modulation of electrode potential	External	EMIRS	Bewick [2, 5]
	Modulation of incident light polarisation	External	IRRAS	Russell *et al.* [9]
	Fixed wavelength and repetitive potential sweeps	External	LPSIRS	Kunimatsu [10]
Fourier transform	Multiple reflections and difference between accumulated series of interferograms	Internal	MIRFTIRS	Neugebauer *et al.* [11]
	Difference between sequenced series of interferograms	External	SNIFTIRS SPAIRS PDIRS	Pons *et al.* [12] Corrigan *et al.* [13] Corrigan *et al.* [14]
	Modulation of incident light polarisation	External	PM-FTIRRAS	Golden *et al.*[15]
	Multiple reflections and electromodulated interferogram	Internal	FTEMIRS	Ozanam and Chazalviel [16]
	Point-by-point interferogram	External	Time-Resolved FTIR	Daschbach *et al.* [17]

(*) Glossary :

EMIRS Electrochemically Modulated Infrared Spectroscopy
IRRAS Infrared Reflection-Absorption Spectroscopy
LPSIRS Linear Potential Sweep Infrared Reflectance Spectroscopy
MIRFTIRS Multiple Internal Reflection Fourier Transform Infrared Spectroscopy
SNIFTIRS Subtractively Normalised Interfacial Infrared Reflectance Spectroscopy
SPAIRS Single Potential Alteration Infrared Reflectance Spectroscopy
PDIRS Potential Difference Infrared Reflectance Spectroscopy
PM-FTIRRAS Polarisation Modulated Fourier Transform Infrared Reflectance Spectroscopy
FTEMIRS Fourier Transform Electro-Modulated Infrared Spectroscopy

2.5.1.Techniques coupled with dispersive instruments

(*i*) EMIRS

This powerful technique makes use of a conventional grating spectrometer. It is based on the interaction of a p-polarised IR beam with a metallic surface which potential is modulated between two limits (the lower potential, E_1, at which the reflectivity is R_1, and the upper potential, E_2, at which the reflectivity is R_2), with a square pulse of 50 to 500 mV amplitude and a frequency of a few hertz. By synchronous analysis of the resultant signals, *i.e.*, the modulated reflectivity, it is possible to reject the non-modulated information (due to absorption by species in the electrolytic solution) and to amplify the signal-to-noise ratio of the absorption bands due to vibration of adsorbed species. The *dc* output of the phase-sensitive detector, $\Delta R(\bar{\nu})$, at a wavenumber $\bar{\nu}$, is then stored, averaged if necessary, and divided by the electrode reflectivity $R(\bar{\nu})$ in order to obtain the spectrum in its final dimensionless form ($\Delta R/R$, $\bar{\nu}$).

Various theoretical forms are to be expected for the EMIRS signal depending on whether species which absorb the radiation do so only at one or at two potential limits (Fig. 8).

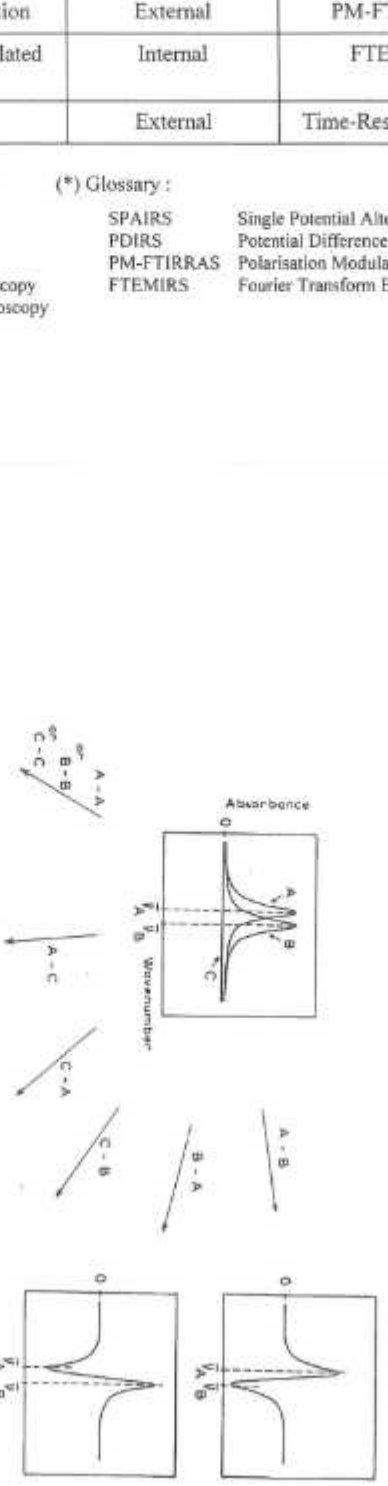

Figure 8. Examples of possible shapes of EMIRS bands.

According to the various limiting cases, the EMIRS signal may appear as a single band, with either a positive sign (from species present in excess at potential E_2) or a negative sign (from species present in excess at potential E_1), a bipolar band (with positive and negative lobes, from species adsorbed at the two potential limits) resulting from bands which shift with potential (Fig. 9), or even not at all if at constant coverage of the adsorbed species, the change of potential does not sufficiently affect the force constant of the bond. The way the species is adsorbed on the surface (*i.e.*, flat or perpendicular) is also a dominant factor governing whether absorption of the radiation occurs. Shifts in band maximum with potential at constant coverage are very common for adsorbed

species and they provide valuable information on the nature of adsorbate-substrate bonding and hence also additional data on adsorbate orientation.

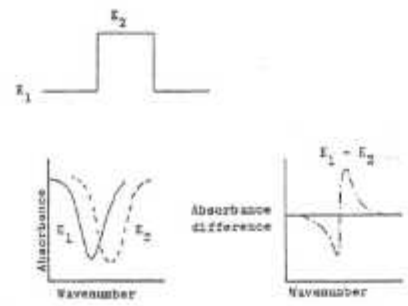

Figure 9. Origin of a bipolar band.

The high sensitivity of EMIRS, as well its ability to reject signals from bulk species has long been demonstrated and has provided valuable structural information on many types of adsorbates. From this point of view it is a unique tool for investigation on the field of electrocatalysis, still competing with the more recent and more sophisticated techniques derived from the use of FTIR spectroscopy. While these techniques are all faster and easier to use than EMIRS, they do not discriminate so easily between surface and solution species.

However, despite its advantages, EMIRS suffers from some inconveniences. The more important one is that the electrode potential is not fixed at a given value, because of potential modulation, so that many electrochemical processes may occur in the potential range of modulation, leading to highly complex EMIRS spectra. The second one is that the modulation technique combined with the so-called *Stark effect* (shift of frequency with potential) leads in most cases to signals having a pseudo-derivative shape, which makes it difficult to extract quantitative information. On the other hand the accurate location of band centres, information which is essential for the qualitative identification of adsorbates, is often problematic because of the different shapes that the bands can exhibit. This point is especially critical when characteristic vibrations are known from transmission studies to adsorb at very close frequencies (*i.e.*, the C=O vibrations of various functional groups), although the signals are obviously detected. The third one is that owing to the use of a spectrometer with a conventional monochromator, the energy throughput is relatively low and the scanning time relatively long. Because of various drifts (either from spectral or electrochemical origins), spectral accumulations cannot be extended to more than a few tens of scans and averaging techniques cannot be used so extensively as with FTIR techniques. Thus, EMIRS signals often remain noisy, which makes their characterisation more difficult, particularly when they have a non-symmetrical or a complex line shape.

To solve these points the integration of EMIRS bands [18] is extremely helpful since it makes their characterisation much easier (better determination of its band centres). Furthermore, the great advantage of noise reduction, which originates from the integration technique, makes the spectra much more convincing, especially when M-shaped bands occur in "noisy" spectral regions. The technique is particularly useful for differentiating the case where a given species has two close absorption bands, or components, from that when two different species have bands at close frequencies and signs which can be opposite (one species being produced, the other being consumed). Qualitative determinations are greatly helped by this technique but quantitative determinations remain difficult as with normal EMIRS spectra.

(*ii*) Other techniques

With the same basic modular equipment, it is possible to set up other types of techniques. One is IRRAS in which the radiation is modulated between parallel and perpendicularly polarised components with a high frequency photoelastic modulator. In this method the signal is obtained as a true IR band. This technique has a good sensitivity and is very useful to confirm EMIRS results by quantitative measurements and to obtain conformational information with respect to the orientation of adsorbates, but for several experimental reasons it is somewhat hard to use.

Another one is I.PSIRS, which allows the investigation, at fixed wavelengths, of the species produced at different electrode potentials during the voltammetric sweep. In this method, repetitive experiments at very close wavelengths allow to build tri-dimensional diagrams [$\Delta R/R$, E, $\bar{\nu}$], *i.e.*, the so-called "reflectograms", which contain the dependence of the spectra on the potential. However, the technique suffers from the very long spectral accumulation times necessary for improving the signal-to-noise ratio and has to be restricted to investigations over very narrow ranges of wavenumbers as well as to very stable electrochemical systems.

2.5.2. Techniques coupled with Fourier Transform spectrometers

(*i*) SNIFTIRS

This technique consists in alternatively collecting successive series of four to eight interferograms at each of the two potential limits E_c and E_a where the reflectivities are R_c and R_a, respectively. These potentials are chosen according to the electrochemical behaviour of the system under study. After Fourier transformation [$\Delta R/R$, $\bar{\nu}$], spectra are obtained by a subsequent subtraction of the co-added series and rationing to R (taken as R_c or R_a). The step between E_c and E_a is repeated until the desired signal-to-noise ratio is obtained (an average of 100 scans is generally sufficient to extract signals of 10^{-5} absorbance unit amplitude). The successive storage of interferograms at E_c and E_a allows drifts, whatever their electrical or chemical origin, to be minimised. Thus, long-duration experiments are possible, up to several hours. Typically, 50 interferograms are stored in a few minutes at each potential limit.

The SNIFTIRS technique has proved to be quite suitable for the *in situ* detection of either electrogenerated intermediates in the double layer or species adsorbed at the electrode surface.

Substances formed at a given potential give rise to a diminution of the reflected intensity as compared with that at the reference potential. As a consequence, the relative reflection band presents a minimum (negative going band). On the contrary, the reflected intensity for substances consumed at a given potential present a maximum (positive going band).

By comparing spectra recorded separately with p- and s-polarised lights it is possible to distinguish the surface species from the solution species. At high incidence angles, the solution species, due to their random orientation, absorb the light in the two polarisation states. In contrast, the surface species, due to the application of the "surface selection rule", absorb the p-polarised light (provided that the dipole moment oscillates in the normal to the surface) but not the s-polarised light which is inactive by cancellation of the s-polarised electric field vectors upon reflection.

Due to computer facilities and to the incredible advances in FTIRS, SNIFTIRS is relatively easier to use than EMIRS and has become a nearly routine technique for investigations at the electrode|solution interface. However, it must be said that the technique still suffers from the difficulty to separate the contribution of solution species, whose consumption (when non-compensated because of mass transport limitations) leads to so strong "negative peaks" in the spectra that the weaker absorption bands of surface species can be masked. Such a difficulty is avoided with EMIRS, where potential modulation eliminates the non-modulated information associated with solution species.

(*ii*) SPAIRS

This technique is a variant of SNIFTIRS, which uses subtractions between series of spectra accumulated at the same potential, but at various times, in order to follow the time dependence of species generated at the electrode surface or accumulated in its vicinity in electrocatalytic reactions. Generally the reflectivities are obtained during very slow voltammetric scans (1 mV s^{-1}), each 100 mV and spectra are calculated as $(R - R_{ref})/R_{ref}$, with the reference spectrum being taken at the adsorption potential. The SPAIRS spectra usually show down-going bands and up-going bands which have to be interpreted in terms of reactive intermediates, poisoning species and reaction products either adsorbed at the electrode surface or desorbed into the solution.

Both SPAIRS and SNIFTIRS techniques allow to detect adsorbed species and reaction products near the electrode surface. However SPAIRS is more suitable for detecting reaction products near the electrode surface, and SNIFTIRS is more suitable for detecting adsorbed species.

(*iii*) Other techniques

PM-FTIRRAS is a variant of SNIFTIRS that uses FTIR spectroscopy with light polarisation. A double modulation technique is employed, using a photomodulator working at high frequency (78 kHz) and a polariser, both inserted in the optical path. This technique has a very high sensitivity, due to the use of high modulation frequencies, which allows reduction of the spectral accumulation times. At the same signal-to-noise ratio, typical accumulation times are notably shorter than in SNITIRS, but to the expense of simplicity.

MIRFTIRS uses a multiple internal reflection cell and it is only a subtraction between accumulated series of spectra taken at various successive potentials (using one of them, usually the first, as a reference), being less sensitive to submonolayers than SNIFTIRS. MIRFTIRS is particularly suitable for following the growth of superficial layers either oxides or organic polymers on electrode surfaces, and also for the identification of products accumulated in the vicinity of the electrode surface since for these two applications less sensitivity is required. As in PM-FTIRRAS, the main difficulty remains on the separation of the contributions of surface species from the solvent contribution. FTEMIRS seems to solve the problem of the solution bands by combining the advantages of interferometry with those of potential modulation, since the interferogram itself is electromodulated.

These techniques have been proven to be useful for studies involving :

- The identification and reactions of adsorbed and non-adsorbed electrochemical reaction intermediates, both neutral and ionic.
- The surface bonding, intermolecular interaction, and dynamics of adsorbates and the effects of electrical fields on these properties.
- Monitoring the potential-dependent concentrations of molecular and ionic species, both adsorbed and in the electric double layer.

Studies of this kind have been made at many types of electrodes, including well-defined single crystals, chemically modified surfaces, semiconductor electrodes, and a number of polycrystalline metal electrodes.

About one and half decades after its beginning we can state that *in situ* IR spectroscopy in the *mid* infrared region (~600 – 400 cm^{-1}) is approaching its maturity as attested by the ability to establish the nature of adsorbed species, the binding site occupancy, lateral couplings and interactions with the electric field and double layer components. In between, the development of the new generation, *in situ far* infrared spectroscopy (below 600 cm^{-1}), overcoming the rather low intensity of conventional laboratory sources and the strong absorption of IR radiation by water, has started and promises to open up new opportunities for investigation in many fields, and attempts have already been made to study electrochemical systems [19].

3. Applications to Electrocatalysis

In electrocatalytic reactions intermediates are frequently chemisorbed species. Reaction rates and mechanisms can vary from one electrode material to another since adsorbed intermediates at some surfaces may in some instances "poison" the electrode surface and ihnibit electrocatalysis. For example, anodic oxidation of small organic molecules, such as methanol, formic acid or formaldehyde, which are of interest in fuel cells, leads to adsorbed intermediate species that can lower reaction efficiency at platinum electrodes, by blocking active sites. In addition, reactants and/or products may be chemisorbed and the reaction rate affected.

The nature of adsorbates bonding to the surface, and interactions of adsorbates with other adsorbed species and solution species, may be conveniently studied by *in situ* infrared spectroelectrochemical techniques.

3.1. Electrooxidation of methanol on platinum electrodes in acid medium

The mechanism of methanol oxidation in platinum electrodes has been the subject of numerous studies, at least the last three decades, leading to a long controversy on the nature of the strongly adsorbed intermediates resulting from the dissociative chemisorption of methanol.

The development of *in situ* IR spectroscopic techniques has allowed a significant progress in the identification of the adsorbed species (reactive and poisoning species) and of the reaction intermediates, making obsolete many of the older works, as well as the reaction mechanisms based only on electrochemical measurements.

The following main points seem to be now widely accepted:

- Different adsorbed species exist simultaneously on the electrode surface, and their chemical nature and surface distribution depends greatly on the surface structure, on the bulk methanol concentration, on the adsorption time, and on the electrode potential.
- The decrease of the current densities with time is due to poisoning effects of adsorbed residues coming from the dissociative adsorption of methanol. The species responsible for the electrode poisoning is adsorbed CO, linearly-, bridge- or multi-bonded to the electrode surface.

EMIRS studies [4, 20 – 22] have allowed the assignment of the main bands of EMIRS spectra to well-defined adsorbed species (see Tables 2 and 3).

Table 2 - Band location of CO_{ads} species.

Band location / cm^{-1}	Type of adsorbed CO
≈ 1865	Multi-bonded CO (CO_M)
≈ 1935-1950	Bridge-bonded CO (CO_B)
≈ 2025-2060	Linearly-bonded CO (CO_L)

Fig. 10 shows that the EMIRS spectra recorded with a relatively low concentration of methanol (in order to decrease the chemisorption rate and thus the amount of poisoning species) have a relatively good signal-to-noise ratio, even after one single unaveraged scan, allowing to distinguish several IR bands, either in the upper wavenumber range or in the lower one. Increasing the accumulation time necessary to average the successive scans leads to a great improvement of the signal-to-noise ratio but the more time required makes the surface distribution of adsorbed species to change as a consequence of the slow adsorption kinetics and of surface rearrangement among

them. It is obvious that the amount of adsorbed CO (both linearly and bridge-bonded to the surface) increases, whereas the intensity of the other IR bands decreases, meaning that adsorbed CO is replacing the other adsorbed species resulting from CH_3OH chemisorption and tends to cover the whole catalytic surface (poisoning phenomena).

The presence of a relatively intense band at 2340 cm^{-1}, even at the first scan, arising from adsorbed CO_2, is surprising since the upper potential limit (0.4 V/RHE) is below the potential of the oxidation region of the platinum surface. This may prove that a direct interaction between the adsorbed methanol residues and the water molecules may lead to oxidation to CO_2. The change of shape and side of this EMIRS band with the accumulation time certainly means that CO_2 is produced at low potentials, both from CO and from other adsorption residues of other adsorbed species.

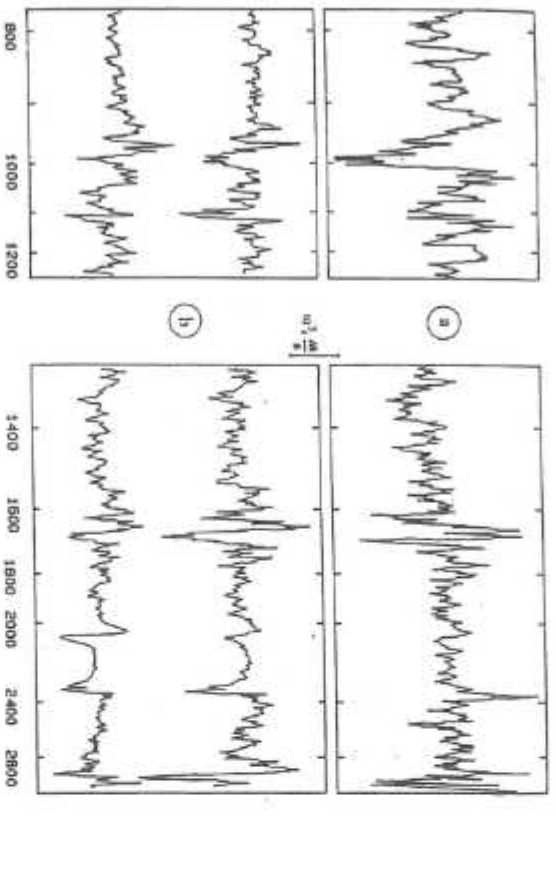

Figure 10. EMIRS spectra of the species resulting from adsorption of methanol (5×10^{-3} M in 0.5 M $HClO_4$) on a polycrystalline platinum electrode for different accumulation times (ΔE = 400 mV, $\bar{E}$ = 0.2V/RHE, f = 13.5 Hz, room temperature): (a) 1st scan, (b) 10th and 25th scans.

Fig. 11 shows that when fairly concentrated methanol solutions are used, the fast chemisorption of CH_3OH on platinum leads to a higher coverage in $CO_{(ads)}$ species than when the concentration of methanol is decreased. Lowering the methanol concentration allows maximum coverage by reactive species without leading to a too rapid poisoning by $CO_{(ads)}$ species during the time-scale of the experiment, but it also leads to noisier EMIRS spectra, which are more difficult to interpret. This figure also shows that in integrated spectra the bands are clearly pointed and, owing to noise reduction, they are well characterised.

Table 3 - EMIRS bands in the spectral range [500 – 3000 cm^{-1}] and tentative assignments for the different species resulting from CH_3OH adsorption on platinum.

Observed EMIRS bands for CH_3OH species ($\bar{\upsilon}$ / cm^{-1})	Reference wavenumbers (from literature)								
	Assignment	Pt–OH	Pt–OH	$CH_3OH_{(ads)}$	$CH_3O_{(ads)}$	$HCOO_{(ads)}$	$CO_{(ads)}$	$CHO_{(ads)}$	Other adsorption
535	δ(OH)		550						
600	δ(OCO)			680					
770	δ(Pt–OH)	1015			760–770				
1025 to 1070	δ(CO) π(C–H)			980	1000	1073			
1070 to 1200									anion adsorption
1320 to 1330	υ_s(OCO)					1330–1340			
1360 to 1480	δ(CH_3) δ(CH)			1380	1430	1377		1390?	
1620	δ(H–OH)		1625						
1650	υ_a(OCO)					1640			
1609 to 1720	υ(C=O)							1700	$COOH_{(ads)}$
1850 to 2060	CO_M, CO_B, CO_L						1875 2060		
2350	υ_a(OCO)								$CO_{2(ads)}$
2635 2825 2925	υ(CH)			2910	2910	2900 (possibly split)		2700–2750 2800–2900	

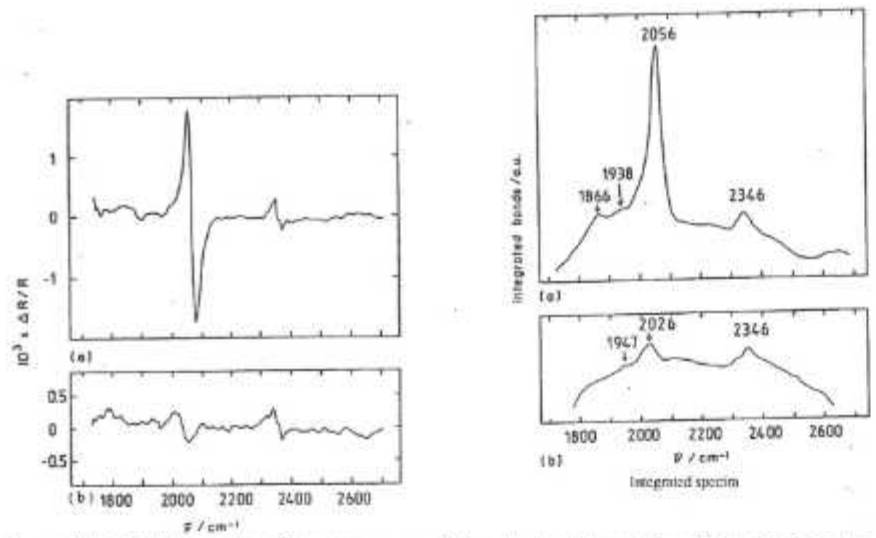

Figure 11. EMIRS spectra, after one scan, of the adsorbed layer formed by chemisorption of methanol in 0.5 M $HClO_4$, with (a) 10^{-1} M CH_3OH, (b) 10^{-3} M CH_3OH, at a polycrystalline platinum electrode; $\Delta E = 300$ mV, $\overline{E} = 0.3$ V/RHE, $f = 13.5$ Hz.

Fig. 12 shows the structure dependence of the electrocatalytic oxidation of methanol [4]. Pt(110) is the most active plane but also the most sensitive to poisoning, which leads to a rapid decrease in the current densities observed. The Pt(111) plane appears to be less sensitive to poisoning phenomena, even though the current densities are rather weak. Finally, the Pt(100) plane is totally blocked over a wide range of potentials, but the current increases sharply once the adsorbed blocking species are removed at higher potentials, the maximum current densities remaining very stable with time. EMIRS spectra confirm these structural effects. The reactive intermediate $(CHO)_{ads}$ was clearly observed in the case of Pt(111), while adsorbed CO was observed for all three surface orientations. However, linearly bonded $CO_{(ads)}$ was the only species detected on Pt(110), whereas two kinds of CO (linearly and bridge-bonded) were clearly present on Pt(100). The latter observation is very interesting, because it is an indication that the blocking phenomena observed with the Pt(100) plane can result from lateral interactions between these two kinds of adsorbed CO species.

The fact that the Pt(111) electrode surface is much less sensitive to poisoning phenomena might make it interesting as an electrode for prolonged utilisation. The exact deactivation process of the (111) surface during methanol oxidation can be expected to differ from that on polycrystalline platinum because of the high superficial density of ternary system crystallographic sites.

EMIRS spectra for methanol electrooxidation on polycrystalline platinum and on Pt(111), in perchloric acid medium, show strong similarities between the two series (Fig. 13).

At one scan, there is a positive contribution below 1700 cm^{-1}, particularly obvious with the Pt(111) electrode, as well as negative contributions at *ca.* 1470 and 1730 – 1740 cm^{-1}. When the number of scans increases, negative contributions increase, so that a strong band at 1564 cm^{-1} is more clearly seen with the polycrystalline than with the single crystal electrode.

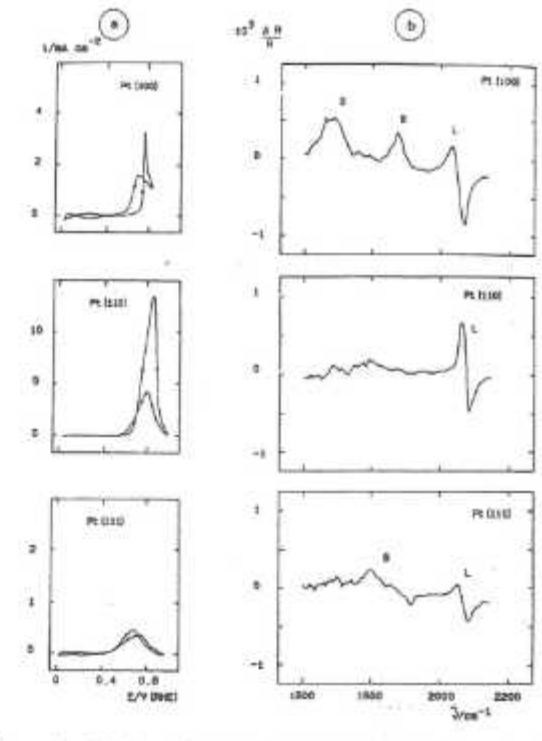

Figure 12. Adsorption and oxidation of 0.1 M CH_3OH in 0.5 M $HClO_4$ at the three low-index faces of Pt single crystals (room temperature): (a) voltammograms (0.05 V s^{-1}; first sweep); (b) EMIRS spectra ($\Delta E = 400$ mV ; $\overline{E} = 0.35$ V/RHE).

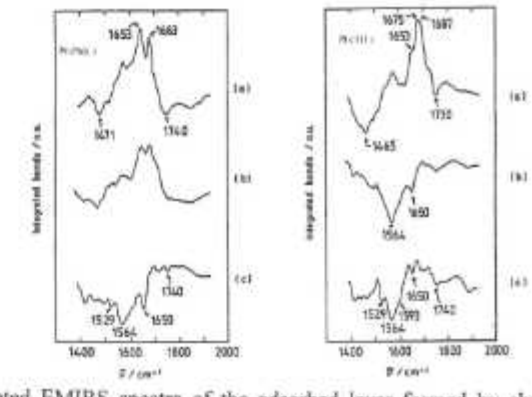

Figure 13. Integrated EMIRS spectra of the adsorbed layer formed by chemisorption of 10^{-3} M CH_3OH at a polycrystalline platinum and at a Pt(111) single crystal electrode, in 0.5 M $HClO_4$; ΔE = 300 mV, $\overline{E}$ = 0.3V/RHE, f = 13.5 Hz: (a) one scan, (b) three scans, (c) five scans.

Changing the applied potential also affects the adsorbed layer, as it is exemplified in Fig. 14 for the polycrystalline platinum electrode.

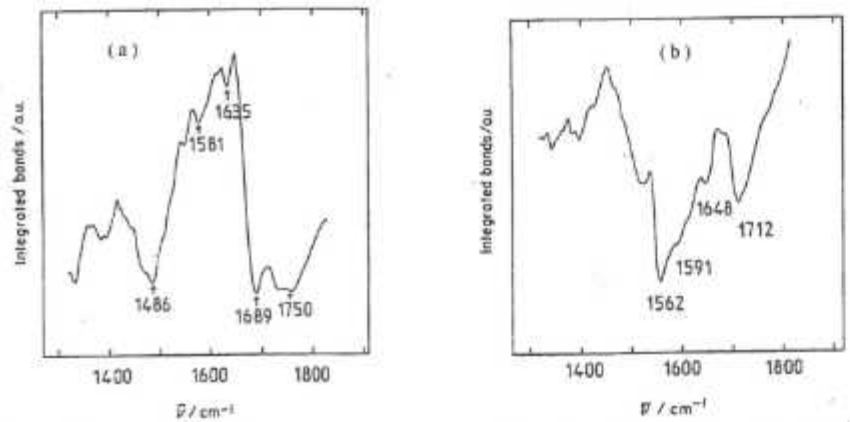

Figure 14. Integrated EMIRS spectrum of the adsorbed layer formed by chemisorption of 10^{-3} M CH_3OH at a polycrystalline platinum electrode, in 0.5 M $HClO_4$ at: (a) $\overline{E}$ = 0.1 V/RHE , (b) $\overline{E}$ = 0.5V/RHE; (ΔE = 300 mV, f = 13.5 Hz, five scans recorded after 30 min.).

The spectral region 1400 – 1900 cm^{-1} is very rich, including all the contributions of the >C=O stretching modes. Comparison of the integrated EMIRS bands of methanol adsorbates on platinum with those of the adsorbates resulting from formic acid, formaldehyde and methyl formate, under strictly similar experiments (Fig. 15 and Fig. 16), allows to discriminate between the different adsorbates of methanol, since the integrated EMIRS bands due to the >C=O stretches of the stable chemisorbed residues of the reference series are well defined and well separated, and thus, characterised (Table 4), allowing the spectral discrimination of adsorbates occurring in the course of these kind of electrocatalytical reactions.

Table 4 - Characteristic vibration wavenumbers, in the range 1440 – 1900 cm^{-1}.

Band location / cm^{-1}	Type of adsorbate
≈1750	Acid group (monomer type)
1690 – 1720 (and higher)	Aldehydic group
1685	Ester
1660 – 1670	Acid group (dimer type)
1630 – 1640	Formate, linked by one O atom
1560 – 1590	Formate anion
1440 – 1460	Methylene group

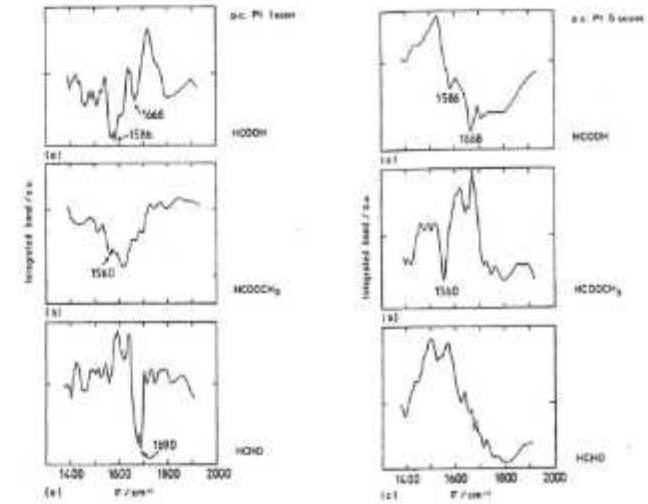

Figure 15. Integrated EMIRS spectra for the adsorbed layer formed by chemisorption at a polycrystalline Pt electrode of (a) 10^{-3} M HCOOH, (b) 10^{-3} M $HCOOCH_3$ and (c) 10^{-3} M HCHO, in 0.5 M $HClO_4$; ΔE = 300 mV, $\overline{E}$ = 0.3V/RHE, f = 13.5 Hz.

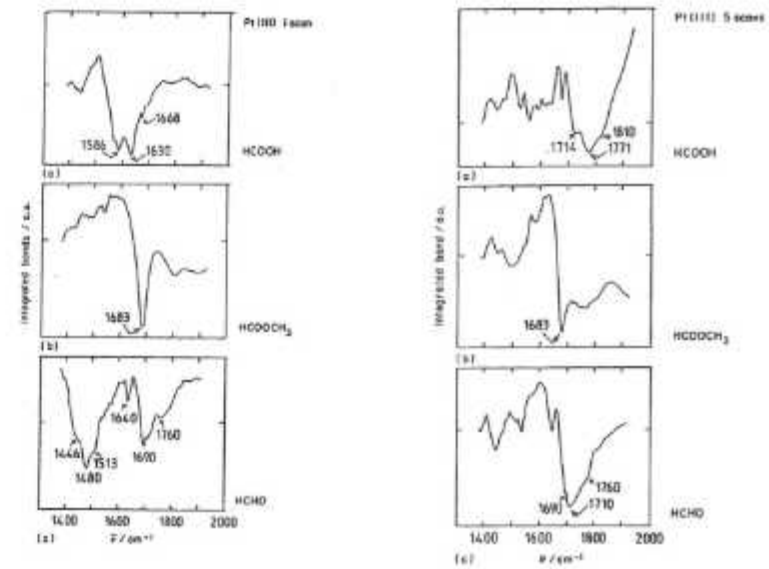

Figure 16. Integrated EMIRS spectra for the adsorbed layer formed by chemisorption at a Pt(111) single crystal electrode of (a) 10^{-3} M HCOOH, (b) 10^{-3} M $HCOOCH_3$ and (c) 10^{-3} M HCHO, in 0.5 M $HClO_4$; ΔE = 300 mV, $\overline{E}$ = 0.3V/RHE, f = 13.5 Hz.

The presence of methyl formate, at least during the initial stages of the methanol chemisorption process on the Pt(111) surface (Fig. 13), and which later on desorbs, may result from a surface reaction taking place between formyl (·CHO) and methoxy (CH_3O·) species, which coexist at the initial surface coverage of the platinum electrode:

$$Pt\text{–}(CHO)_{ads} + Pt\text{–}(CH_3O)_{ads} \rightarrow Pt\text{–}(HCOOCH_3)_{ads} \rightarrow HCOOCH_{3(aq)}$$

Scheme 1

Acid groups are also produced, probably as -COOH or dimers, and possibly formate anions.

These later species, by surface competition, dominate after five scans or at high potentials, but some formyl species still remain on the surface. This explains why formic acid and formaldehyde were detected as secondary reaction products in solution, in addition to CO_2, which remain the main oxidation product [23]. On the other hand, $CO_{(ads)}$ species are slowly but irreversibly formed, specially the multi-bonded species on Pt(111) (~1885 cm^{-1}).

The presence of methyl formate in the bulk of the solution was confirmed by SNIFTIRS measurements [24]. It could result from a solution reaction, as well, and adsorption would be possible by equilibrium with the solution species:

$$(CH_3OH)_{aq} + HCOOH_{(aq)} \longrightarrow HCOOCH_{3(aq)} + H_2O$$

$$(HCOOCH_3)_{aq} \longleftrightarrow Pt\text{–}(HCOOCH_3)_{ads}$$

Scheme 2

However this should take time, as methyl formate would have to reach an appreciable concentration in solution before displacing the equilibrium towards the formation of the correspondent adsorbed species. Therefore, the fact that it is initially detected on the surface certainly argues in favour of the direct surface reaction (Scheme 1).

On the basis of all these observations and conclusions, it is possible to establish a probable way of bonding to platinum surfaces of the detected adsorbed species (Fig. 17), as well as a detailed mechanism for the oxidation of methanol in platinum in acid medium (Scheme 3).

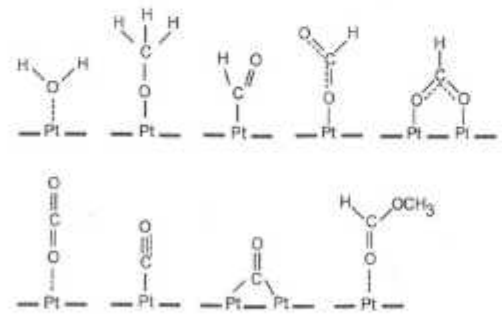

Figure 17. Probable bonding of adsorbate species to platinum resulting from the electrooxidation of CH_3OH in acid medium.

(1) $Pt + H_2O \longrightarrow Pt - (OH)_{ads} + H^+_{ads} + e^-$

(2) $Pt + (CH_3OH)_{sol} \longrightarrow Pt - (CH_3OH)_{ads}$

(3) $Pt - (CH_3OH)_{ads} \longrightarrow Pt - (CH_3O)_{ads} + H^+_{aq} + e^-$

(4) $Pt - (CH_3O)_{ads} \longrightarrow Pt - (CH_2O)_{ads} + H^+_{aq} + e^-$

(5) $Pt - (CH_2O)_{ads} \longrightarrow Pt - (CHO)_{ads} + H^+_{aq} + e^-$

(6a) $Pt - (CHO)_{ads} \longrightarrow Pt - (CO)_{ads} + H^+_{aq} + e^-$

(6b) $Pt - (CHO)_{ads} + Pt - (OH)_{ads} \longrightarrow 2Pt + CO_2 + H^+_{aq} + e^-$

(6c) $Pt - (CHO)_{ads} + Pt - (OH)_{ads} \longrightarrow Pt + Pt - (COOH)_{ads} + H^+_{aq} + e^-$

(7a) $Pt - (CO)_{ads} + Pt - (OH)_{ads} \longrightarrow 2Pt + CO_2 + H^+_{aq} + e^-$

(7b) $Pt - (CO)_{ads} + Pt - (OH)_{ads} \longleftrightarrow Pt + Pt - (COOH)_{ads}$

(8) $Pt - (COOH)_{ads} \longrightarrow Pt + CO_2 + H^+_{aq} + e^-$

Scheme 3

The key point is the formation of the reactive intermediate $(CHO)_{ads}$ and its further oxidation, which can be summarised in Scheme 4:

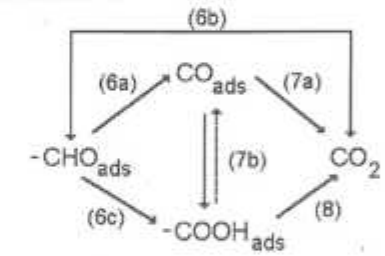

Scheme 4

From this Scheme, it is possible to understand the requirements for the use of methanol in a fuel cell in acid medium. It is necessary to avoid the formation of $(CO)_{ads}$ and to favour route (6b), leading directly to CO_2, or alternatively the indirect routes (6c) and (8) through $(COOH)_{ads}$. This is probably possible by using specific surface structures.

3.2. Electrooxidation of D-sorbitol on platinum electrodes in acid medium

In order to get more insight into the oxidation mechanism of D-sorbitol on polycrystalline platinum electrodes, *in situ* IR reflectance spectroscopic studies were conducted by FTIRS (under the SNIFTIRS and SPAIRS variants) and EMIRS [25]. These studies were carried out in order to elucidate the nature of reactive intermediates and reaction products and to follow their dependence on the electrode potential and bulk concentration of D-sorbitol (10^{-3} M to 10^{-1} M).

The superficial concentration of the different types of adsorbed species was found to depend on the concentration of D-sorbitol on the bulk and on the electrode potential. The infrared spectroscopic evidence for CO_{ads} was found by SNIFTIRS and EMIRS, showing that linearly adsorbed CO predominates as strongly bonded adsorbate for higher bulk concentrations of D-sorbitol.

The integrated EMIRS spectra displayed in Fig. 18b indicate that, for 10^{-1} M bulk concentration of D-sorbitol, adsorbed CO appears mainly as CO_L (strong band at 2050 cm^{-1}) with minor contributions of CO_B (bands at 1885 cm^{-1} and 1930 cm^{-1}), while for 10^{-3} M D-sorbitol it appears only as CO_B (two bands at 1890 cm^{-1} and 1935 cm^{-1}).

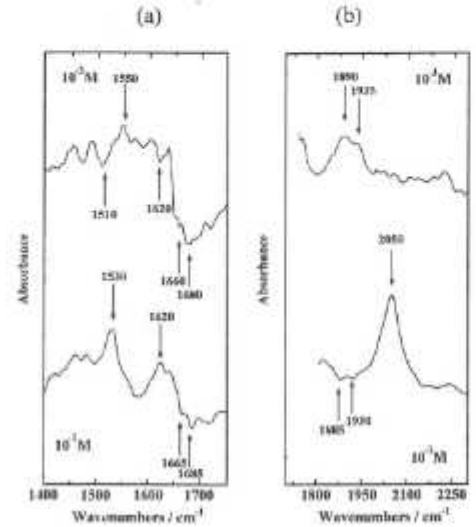

Figure 18. Integrated EMIRS spectra, after five spectral scans, in the range (a) 1400 to 1750 cm^{-1} and (b) 1800 to 2300 cm^{-1}, of 10^{-1} M and 10^{-3} M D-sorbitol in 0.5 M $HClO_4$ at a polycrystalline Pt electrode; (ΔE = 300 mV, $\overline{E}$ = 0.3 V/RHE, f = 13.5 Hz).

A set of the resulting SPAIRS spectra obtained at a platinum electrode for three bulk concentrations of D-sorbitol (10^{-3} M to 10^{-1} M) is shown in Figs. 19a – c.

For 10^{-1} M D-sorbitol (Fig. 19a) and in the so-called carbonyl stretching region, a strong band developed at ≈1780 cm^{-1} is accompanied by a smaller band at ≈1740 cm^{-1}. This strong band could be attributed to the C=O stretch of a saturated γ-lactone (five-membered ring). The band at 1740 cm^{-1}, could be attributed to the carbonyl stretch of a δ-lactone (six-membered ring). These two bands are visible from around +0.6 to +1.2 V/RHE. The presence of these bands, indicates that the two lactone species are the main final products in solution. In contrast, for 10^{-2} M and 10^{-3} M D-sorbitol (Fig. 19b and 19c) no bands are detected in this range. The bands observed in the range 1640 to 1670 cm^{-1} are probably due to the presence of interfacial water (bands also observed in the EMIRS spectra (Fig. 18a), in the range 1620 to 1685 cm^{-1}).

For higher bulk concentrations, 10^{-2} M and 10^{-1} M, (Figs. 19a and 19b), adsorbed CO appears as linearly-bonded CO. These bands are seen from 0.1 to 0.4 V/RHE, in a range from 2000 to 2100 cm^{-1}. After 0.4 V/RHE the adsorbed CO is fully oxidized to CO_2, confirmed by the development of a band at around 2350 cm^{-1}, corresponding to the CO_2 trapped in the thin layer.

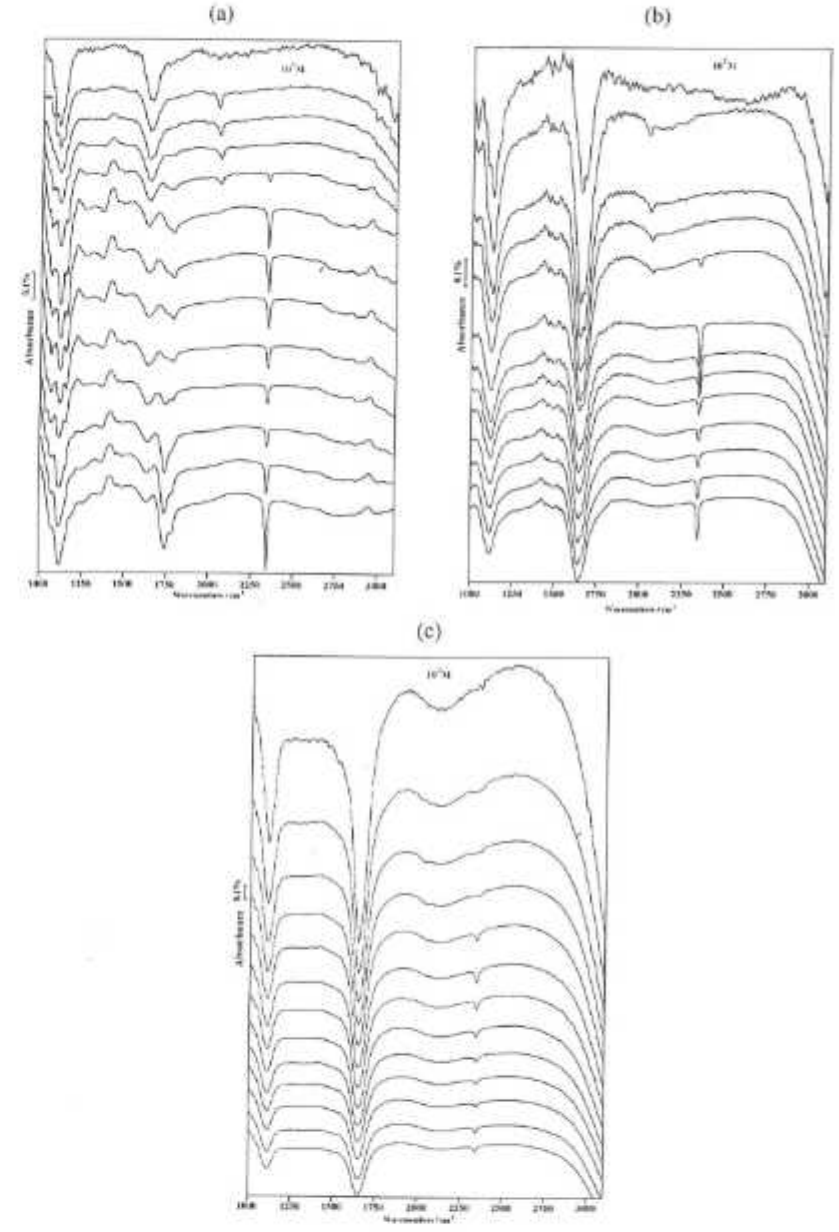

Figure 19. *P*-polarised SPAIRS spectra at various potentials (from 0 to 1.2 V/RHE, each 100 mV) of (a) 10^{-1} M, (b) 10^{-2} M and (c) 10^{-3} M D-sorbitol in 0.5 M $HClO_4$ on a polycrystalline Pt electrode, (spectra are displayed starting from the top of the figure).

EMIRS was also used to study the electrosorption of D-sorbitol on platinum single crystal electrodes in perchloric acid medium [26 – 28]. Recently, these spectroscopic studies, together with Programmed Potential Voltammetry (PPV) were extended to Pt(110) and Pt(111) [28].

The integrated EMIRS spectra, recorded during the electrosorption of D-sorbitol at Pt(111) and Pt(110) electrodes, are shown in Figures 20a and 20b, respectively. The low concentration of D-sorbitol in solution, 10^{-3} M, was chosen to allow maximum coverage by reactive species without leading to a too rapid poisoning by $CO_{(ads)}$ species during the time-scale of the experiment.

A general view of the two spectra allow us to draw some conclusions. After five spectral scans, for Pt(111), $CO_{(ads)}$ species appear mainly as linearly-bonded CO (strong band at 2038 cm^{-1}), while for Pt(110), two $CO_{(ads)}$ species coexist at the electrode surface: linearly-bonded CO (band at 2050 cm^{-1}) and bridge-bonded CO (band at 1973 cm^{-1}). Moreover, multi-bonded $CO_{(ads)}$ species are certainly responsible for the absorption bands located between 1808 cm^{-1} and 1906 cm^{-1} for Pt(110) (Fig. 20b) and at 1812 cm^{-1} and 1830 cm^{-1} for Pt(111) (Fig. 20a).

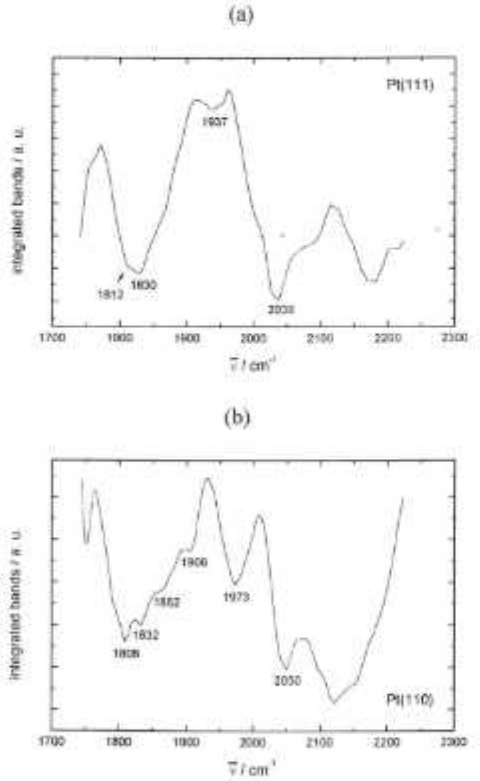

Figure 20. Integrated EMIRS spectra of the adsorbed layer formed by chemisorption of 10^{-3} M D-sorbitol at (a) Pt(111) and (b) Pt(110) electrodes, in 0.5 M $HClO_4$; (ΔE = 300 mV, $\overline{E}$ = 0.3 V/RHE, f = 13.5 Hz, 5th scan).

Experimental data obtained by PPV has shown that, in the case of Pt(111), the main adsorbed species present at the surface for long adsorption times is linearly-adsorbed CO ($N_{eps} \approx 2$), while for

Pt(110) the value oscillates around 1, in a wide range of adsorption times, corresponding to a mixture of different species including multi-bonded and bridge-bonded CO, as confirmed by EMIRS. These species are probably the ones responsible for the strong deactivation of the electrode surface.

3.3. Electrooxidation of D-glucose at platinum electrodes in alkaline medium

SPAIRS and SNIFTIRS have been applied to the investigation of the electrooxidation process of D-glucose at polycrystalline Pt electrodes in NaOH solutions [29]. Various reactive or poisoning intermediates were identified and their potential dependence monitored.

SPAIRS spectra were collected under s or p-polarisation of the IR beam, each 100 mV, between +0.10 V/RHE and +1.60 V/RHE, and more than 30 spectra were thus collected during the forward and backward potential sweep (Fig. 21)

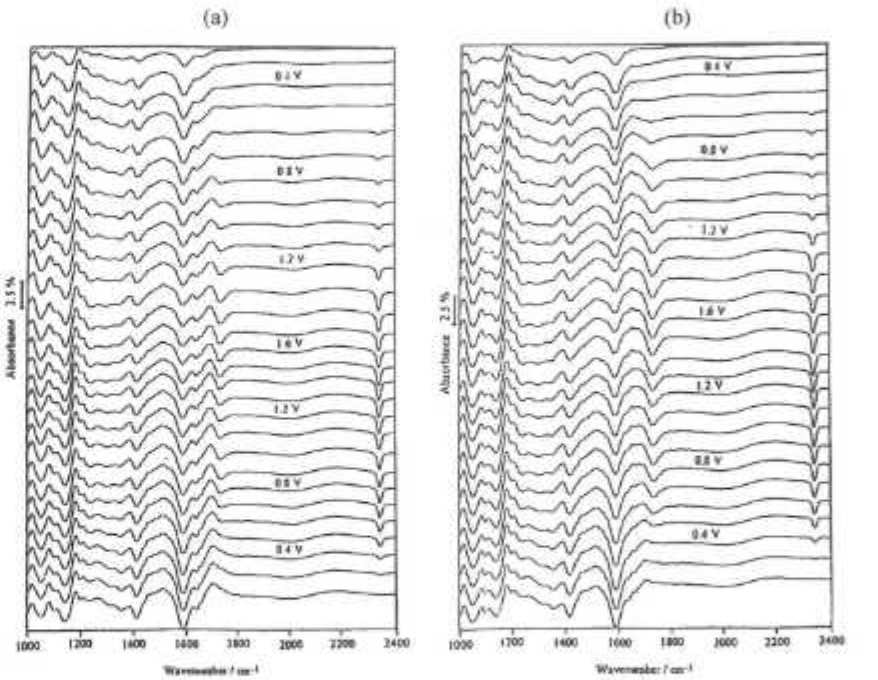

Figure 21. SPAIRS spectra at various potentials of 0.1M D-glucose in 0.1M NaOH, on a polycrystalline Pt electrode (at low temperature); (a) p-polarisation, (b) s-polarisation.

The presence of two bands at around 1413 cm^{-1} (symmetric O–C–O stretching) and 1587 cm^{-1} are due to gluconate formed in the thin solution layer at all over the range of potentials. The intensity of the two bands is potential dependent and , when the second one decreases, there appears a band at ca. 2343 cm^{-1}, due to CO_2 in solution. Two weak additional bands in the range 1180–1250 cm^{-1} indicate that a product having a lactone structure is formed resulting from the electrooxidation of glucose at high potentials. The value of the carbonyl stretch, *ca.* 1732 cm^{-1}, favours the hypothesis of a δ-gluconolactone species, slightly adsorbed at the electrode surface. As soon as the surface is reduced, the lactone form disappears and more gluconate is formed.

SNIFTIRS experiments were carried out under p-polarisation and the corresponding spectra are displayed in Fig. 22.

The set of SNIFTIRS spectra shows that the bands are globally located at the same wavenumbers than in the SPAIRS spectra, but an additional $CO_{(ads)}$ bipolar band is seen, centred near 2040 cm^{-1}, resulting essentially from the technique, whereas the CO_2 band is much less prominent than in SPAIRS experiments, because it is accumulated in the thin layer solution and tends to disappear by diffusion on the bulk solution. The intensity of the symmetric-asymmetric O–C–O stretches of gluconate depends on the potential, which means that it is weakly adsorbed on the surface and not only present on solution. Two configurations are possible for the weakly adsorbed gluconate (Scheme 5). Configuration (I) is favoured at low potentials and configuration (II) predominates when the applied potential is more positive.

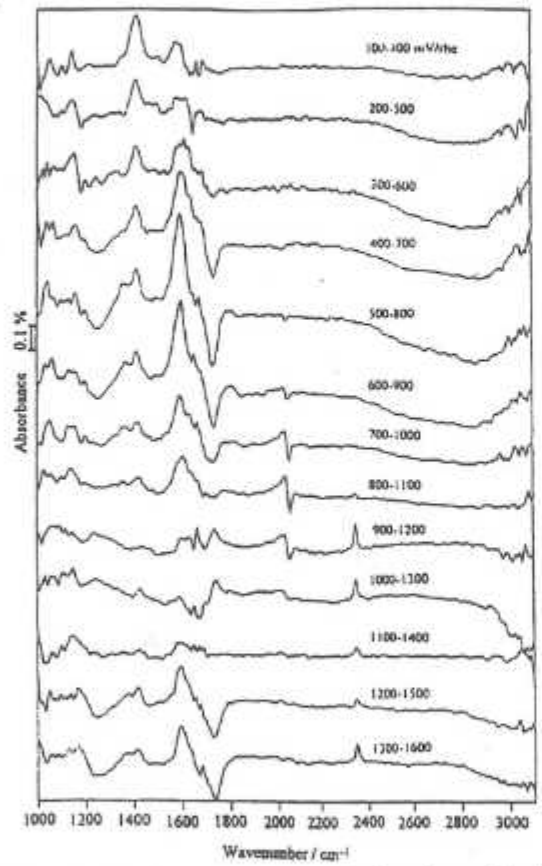

Figure 22. SNIFTIRS spectra at various modulation amplitudes of potential of 0.1M D-glucose in 0.1 M NaOH, on a polycrystalline Pt electrode, at low temperature.

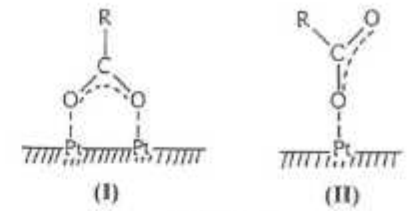

Scheme 5

From the above results it is clear that the SPAIRS and SNIFTIRS techniques are not strictly equivalent and that both have to be operated for a complete investigation of a given problem.

3.4. Electrooxidation of ethanol at iridium and rhodium electrodes in acid medium

SPAIRS has been used to study the electroadsorption and oxidation of ethanol at polycrystalline Ir and Rh electrodes in $HClO_4$ solutions [30] (Figs. 23 and 24).

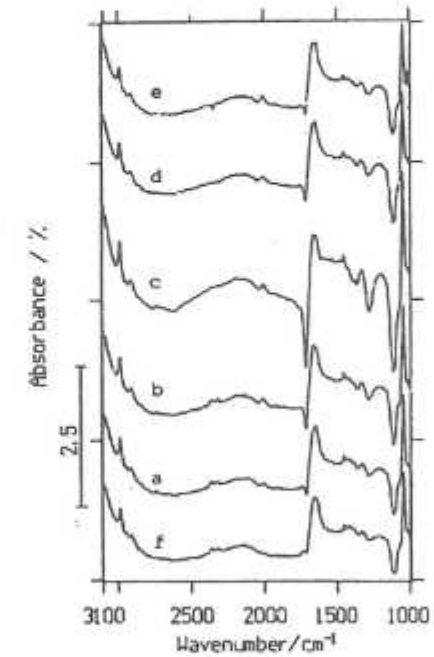

Figure 23. SPAIRS spectra recorded at various potentials, of the surface species on a polycrystalline Ir electrode in 0.5 M $HClO_4$ + 0.5 M C_2H_5OH (difference spectra with the reference obtained at 0.15 V, p-polarisation, 512 interferograms, reverse scan). Potentials: (a) 0.25 V; (b) 0.35 V; (c) 0.55 V ; (d) 0.75 V; (e) 0.95 V; (f) 0.15 V.

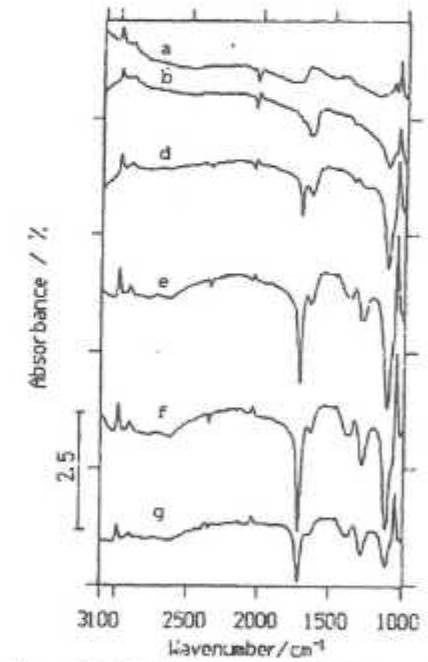

Figure 24. SPAIRS spectra recorded at various potentials, of the surface species on a polycrystalline Rh electrode in 0.5 M $HClO_4$ + 0.5 M C_2H_5OH (p-polarisation, 512 interferograms). Potential windows: (a) [0.05, 0.35 V]; (b) [0.15, 0.45 V]; (c) [0.25, 0.55 V]; (d) [0.35, 0.65 V]; (e) [0.45, 0.75 V]; (f) [0.55, 0.85 V]; (g) [0.65, 0.95 V].

In the potential region of adsorption, adsorbed CO is the main dissociation product detected spectroscopically. However, the adsorbed CO layer has a distinct composition on each metal, and the potential dependence is also different. CO_L is dominant on Ir and remains on the surface up to 0.7 V, whereas CO_L and CO_B are initially formed on Rh. In this latter case, CO_L was found to disappear at more positive potentials than CO_B.

In the electrooxidation region, the two main products are acetic acid and CO_2. However, comparison of the process on Ir and Rh shows that there is less CO_2 produced on Ir than on Rh. Accordingly, more acetic is produced on Ir. Acetaldehyde is mainly formed on Ir when the surface is partially covered by $CO_{(ads)}$ and it lacks in the oxidation products on Rh owing to the existence of bridge sites occupied by CO_B.

The oxidation of ethanol, which can be taken as a test reaction, emphasises an interesting behaviour between two noble metals, which may be relevant for other applications. If the aim to be achieved is the total oxidation of ethanol to CO_2, then Rh is a better catalyst, i.e. more efficient. However, if selectivity is the most important goal, Ir is far more interesting than Rh for the given electrochemical reaction, in that it may lead selectively to either acetaldehyde or acetic acid, essentially without CO_2 as a by-product, depending on the chosen potential.

3.5. Electrooxidation of hipophosphite on nickel electrodes

The electrooxidation of hypophosphite ions on polycrystalline nickel in alkaline solutions has been investigated by SNIFTIRS [31]. Throughout the study, 200 interferograms were collected at each potential. Difference spectra obtained as the potential is varied stepwise from -1.15 V up to -0.80 V are shown in Fig. 25.

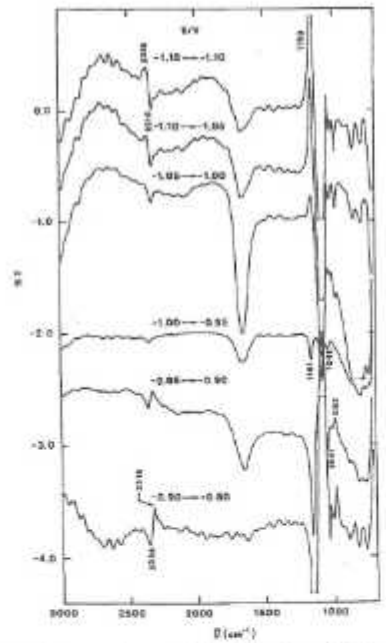

Figure 25. SNIFTIRS spectra for a polycrystalline Ni electrode in 0.1 M NaH_2PO_2 and 0.1 M NaOH.

The main features seen on these spectra are negative bands, at 2318 cm^{-1}, 1080 cm^{-1}, 1027 cm^{-1} and 983 cm^{-1}, due to the formation of phosphite ion, and which increase when the potential is more negative. Further spectral confirmation of this oxidation is the appearance of positive bands at 2356 cm^{-1}, 1161 cm^{-1} and 1041 cm^{-1}, which indicate the depletion of the hypophosphite as it is oxidised to phosphite.

Several other series of spectra were collected and analysed in this study, as a function of the electrode potential during the anodic, cathodic scans and at open circuit potential, as a function of time. Phosphite ions were the only oxidation product to be detected and the hypophosphite ions were found to adsorb on the nickel surface by the two hydrogen atoms at open circuit potential, an orientation which persists until the oxidation takes place (Scheme 6).

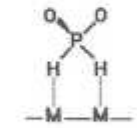

Scheme 6

4. Concluding remarks

In situ IR spectroscopic techniques were discussed and illustrated by a few selected examples. The feasibility of applying these techniques to the investigation of the electrode|electrolyte interface is now firmly established.

Each of the techniques described possesses its own advantages and limits. The most appropriate technique to employ depends on the subject under investigation.

Undoubtedly, many aspects of the techniques can still be improved. For example, more effort is needed both to increase the sensitivity and to extend the wavenumbers range to higher wavenumbers (where combination bands and overtones are expected) and to lower wavenumbers (in the far-infrared range, in order to reach the metal-substrate vibrations).

Acknowledgements

This work was partially supported by international cooperation. We are greatly indebted to a CNRS (France) / JNICT (Portugal) scientific collaboration program. Many thanks are extended to all of the team working at the "Laboratoire de Chimie I, *Electrochimie et Interactions*", University of Poitiers (France), who have much facilitated this work. One of us (L. P.) also acknowledges JNICT (PRAXIS XXI) for the award of a grant.

References

[1] H.B. Mark Jr. and S. Pons, *Anal. Chem.*, 38 (1966) 119.

[2] A. Bewick, K. Kunimatsu and S. Pons, *Electrochim. Acta*, 25 (1980) 465.

[3] B. Beden and C. Lamy, in *Spectroelectrochemistry-Theory and Practice*, R.J. Gale (Ed.), Plenum Press, New York, pp.189-261, (1988).

[4] B. Beden, J.-M. Léger and C. Lamy, in *Modern Aspects of Electrochemistry*, J.O'M Bockris (Ed.), Plenum Press, New York, Vol. 22, pp. 97-264, (1992).

[5] A. Bewick and S. Pons,in Advances in *Infrared and Raman Spectroscopy*, R.J.H. Clark and R.E. Hester (Eds.), Wiley Heyden, London, Vol. 12, pp.1-63, (1985).

[6] J.K. Foley, C. Korzeniewski, J.L. Daschbach and S. Pons, in *Electroanalytical Chemistry*, A.J. Bard (Ed.), Marcel Dekker, New York, Vol. 14, pp. 309-440, (1986).

[7] K. Ashley, Spectroscopy 5 (1990) 22.

[8] T. Iwasita and F.C. Nart, in *Advances in Electrochemical Engineering*, H. Gerischer and C.W. Tobias (Eds.), VCH, Weinheim, Vol. 4, pp. 123-216, (1995).

[9] J.W. Russell, J. Overend, K. Scanlon, M.W. Severson and A. Bewick, *J. Phys. Chem.*, 86 (1982) 3066.

[10] K. Kunimatsu, *J. Electroanal. Chem.*, 140 (1982) 205.

[11] H. Neugebauer, G. Nauer, N. Brinda-Konopik and G. Gidaly, *J. Electroanal. Chem.*, 122 (1981) 381.

[12] S. Pons, T. Davidson, and A. Bewick, *J. Electroanal. Chem.*, 160 (1984) 63.

[13] D.S. Corrigan, M.J. Weaver and W.H. Leung, *Anal. Chem.*, 59 (1987) 2252.

[14] D.S. Corrigan and M.J. Weaver, *J. Phys. Chem.*, 90 (1986) 5300.

[15] W.G. Golden, K. Kunimatsu and H. Seki, *J. Phys. Chem.*, 88 (1984) 1275.

[16] F. Ozanam and J.N. Chazalviel, *J. Electron. Spectrosc. Relat. Phenom.*, 45 (1987) 32.

[17] J. Daschbach, D. Heisler and S. Pons, *Appl. Spectrosc.*, 40 (1986) 489.

[18] B. Beden, *J. Electroanal. Chem.*, 345 (1993) 1.

[19] C.A. Melendres, B. Beden and G.A. Bowmaker, *J. Electroanal. Chem.*, 383 (1995) 191.

[20] B. Beden, F. Hahn, J.-M. Léger, C. Lamy, M.I.S. Lopes, *J. Electroanal. Chem.*, 258 (1989) 463.

[21] M.I.S. Lopes, B. Beden, F. Hahn, J.-M. Léger and C. Lamy, *J. Electroanal. Chem.*, 313 (1991) 323.

[22] M.I.S. Lopes, I.T.E. Fonseca, P. Olivi, .B. Beden, F. Hahn, J.-M. Léger and C. Lamy, *J. Electroanal. Chem.*, 346 (1993) 415.

[23] E.M. Belgsir, H. Huser, J.-M. Léger and C. Lamy, *J. Electroanal. Chem.*, 225 (1987) 281.

[24] T. Iwasita-Vielstich, in *Advances in Electrochemical Engineering*, H. Gerischer and C.W. Tobias (Eds.), VCH, Weinheim, Vol. 1, pp. 128-170, (1990).

[25] L. Proença, M.I.S. Lopes, I. Fonseca, F. Hahn and C. Lamy, (in preparation).

[26] I.T.E. Fonseca, M.I.S. Lopes, L. Proença, B. Beden, J.-M. Léger, F. Hahn and C. Lamy, *Extended Abstracts of the 45th ISE Meeting*, IV-25, vol.2, Porto (1994).

[27] J.-M. Léger, F. Hahn, B. Beden, C. Lamy, M.F. Bento, I. Fonseca and M.I.S. Lopes, *J. Electroanal. Chem.*, 356 (1993) 255.

[28] L. Proença, M.I.S. Lopes, I. Fonseca, J.-M. Léger and C. Lamy, *J. Electroanal. Chem.*, (in press).

[29] B. Beden, F. Largeaud, K.B. Kokoh and C. Lamy, *Electrochimica Acta* , 41 (1996) 701.

[30] N.R. Tacconi, R.O. Lezna, B. Beden, F. Hahn and C. Lamy, *J. Electroanal. Chem.*, 379 (1994) 329.

[31] L.M. Abrantes, M.C. Oliveira, J.P. Correia, A. Bewick and M. Kalaji, *Faraday Transactions*, (in press).